Electronic Supporting Information

High-Efficient Fe-Cu Dual-site Nanoparticles Supported on Black Pearl 2000 carbon as Oxygen Reduction Reaction Catalysts for Al-air Batteries

Kun Liu, Xiaoyue Ye, Angli Zhang, Xiaoyan Wang, Ting Liang, Yan Fang, Wang Zhang, Ke Hu, Xiaowu Liu *, Xin Chen*

Anhui Provincial Laboratory of Biomimetic Sensor and Detecting Technology, College of Materials and Chemical Engineering, West Anhui University, Lu'an 237012, China.

The Koutecky-Levich diagram (J^{-1} vs $\omega^{-1/2}$) was investigated under different electrode potentials. In accordance with the Koutecky-Levich equation, the electron transfer number (n) can be determined by calculating the slope of its linear regression line. The hydrodynamic properties of the prepared sample can be evaluated using the following Koutecky-Levich equation:[1]

$$\frac{1}{j}=\frac{1}{j_L}+\frac{1}{j_K}=\frac{1}{B\omega^{1/2}}+\frac{1}{j_K} \quad \text{Equation (1)}$$

$$B=0.62nFC_0D_0^{2/3}\upsilon^{-1/6} \quad \text{Equation (2)}$$

For the Tafel plot, the kinetic current was calculated as equation (3):

$$j_K=\frac{j\times j_L}{j_L-j} \quad \text{Equation (3)}$$

The experimentally measured current density, denoted as j, is compared to the diffusional-limited current density (j_L) and dynamic current density (j_K). The electrode speed is represented by ω in rad/s. F refers to the Faraday constant (96485 $C\cdot mol^{-1}$), while C_0 (1.2×10^{-3} $mol\cdot L^{-1}$) and D_0 (1.9×10^{-5} $cm^2\cdot s^{-1}$) correspond to the volume

concentration and diffusion coefficient of O_2 in 0.1 M KOH respectively. ν represents the kinematic viscosity of the electrolyte with a value of 0.01 $cm^2 \cdot S^{-1}$. B denotes the K-L graphs.

The rotating ring disk electrode (RRDE) technique was estimated transfer number (n). The equation provided both the electron transfer number (n) and the yield of hydrogen peroxid ($\%H_2O_2$) from the following equations (4-5):[2]

$$\%HO_2^- = 200 \times \frac{I_r / N}{I_d + I_r / N} \quad (4)$$

$$n = 4 \times \frac{I_d}{I_d + I_r / N} \quad (5)$$

Where Id represents disk current, Ir represents ring current, and N represents current collection efficiency of the Pt ring (0.424).

Fabrication and performance evaluation of Al-air batteries.

The electrochemical activity of the catalyst in the aluminum-air battery was investigated by preparing a three-layer air electrode through the hot pressing method, which consisted of a gas diffusion layer, a current collector, and a catalytic layer. The nickel foam serves as the air electrode collector, possessing excellent conductivity and high strength. The catalyst layer was prepared by mixing catalyst, acetylene black, Ketjenblack and polytetrafluoroethylene (PTFE) at a weight ratio of 3:1:3:3, followed by dispersion in ethanol to a homogeneous slurry. Once the slurry reaches a paste-like consistency, it was rolled onto a glass plate until the thickness reached approximately 0.2 mm. The air electrode thickness was compressed to the range of 0.3-0.5mm (3 cm×5 cm) using the roller press (MSK-HRp-MR100A) provided by Hefei Kejing.

Finally to vacuum drying at 60°C for a duration of 12 hours. During the entire battery test, the air electrode are used as the cathode while the polished aluminum electrode functioned as the anode electrodes. A corrosion inhibitor electrolyte consisting of 6mol·L^{-1} KOH, 0.0005mol·L^{-1} $In(OH)_3$, 0.0075mol·L^{-1} ZnO and 0.01mol·L^{-1} Na_2SnO_3 was employed.The constant discharge test was carried out on the Neware battery test system (Shenzhen, China) using the aluminum air battery test device of Youkete New Energy Technology Co., LTD. (OMS-TF1) (Changzhou, Jiangsu, China). The detailed experimental procedures have been described in our previous work.

Supporting Figures

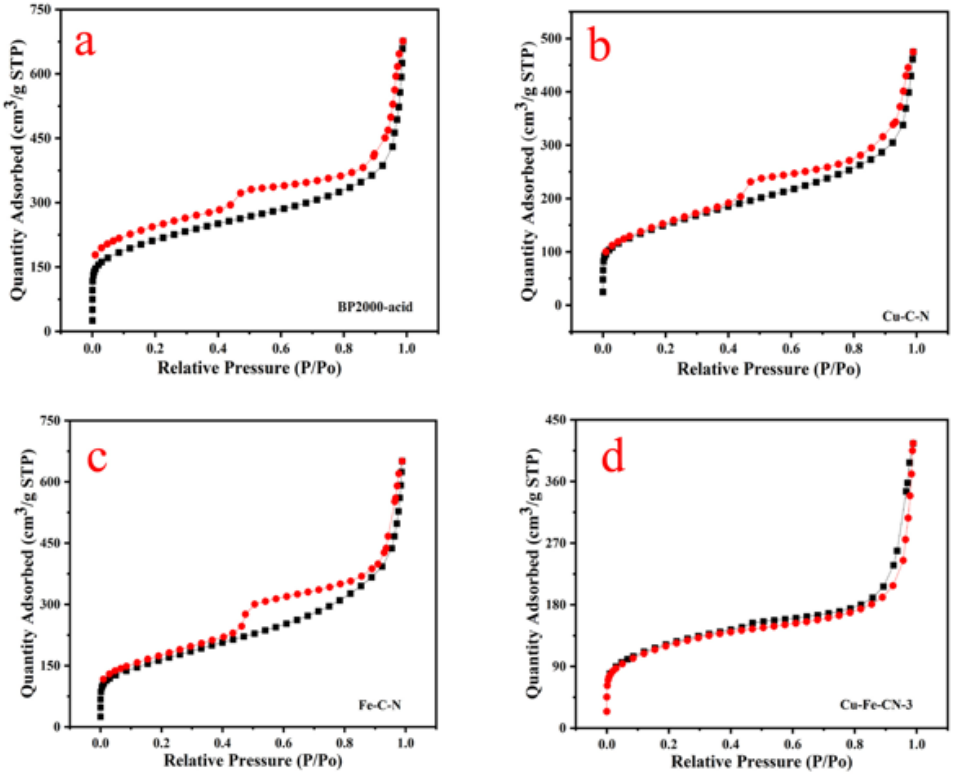

Figure S1. Nitrogen sorption isotherms of the BP2000-acid, Cu-C-N, Fe-C-N and Cu-Fe-CN-3 samples.

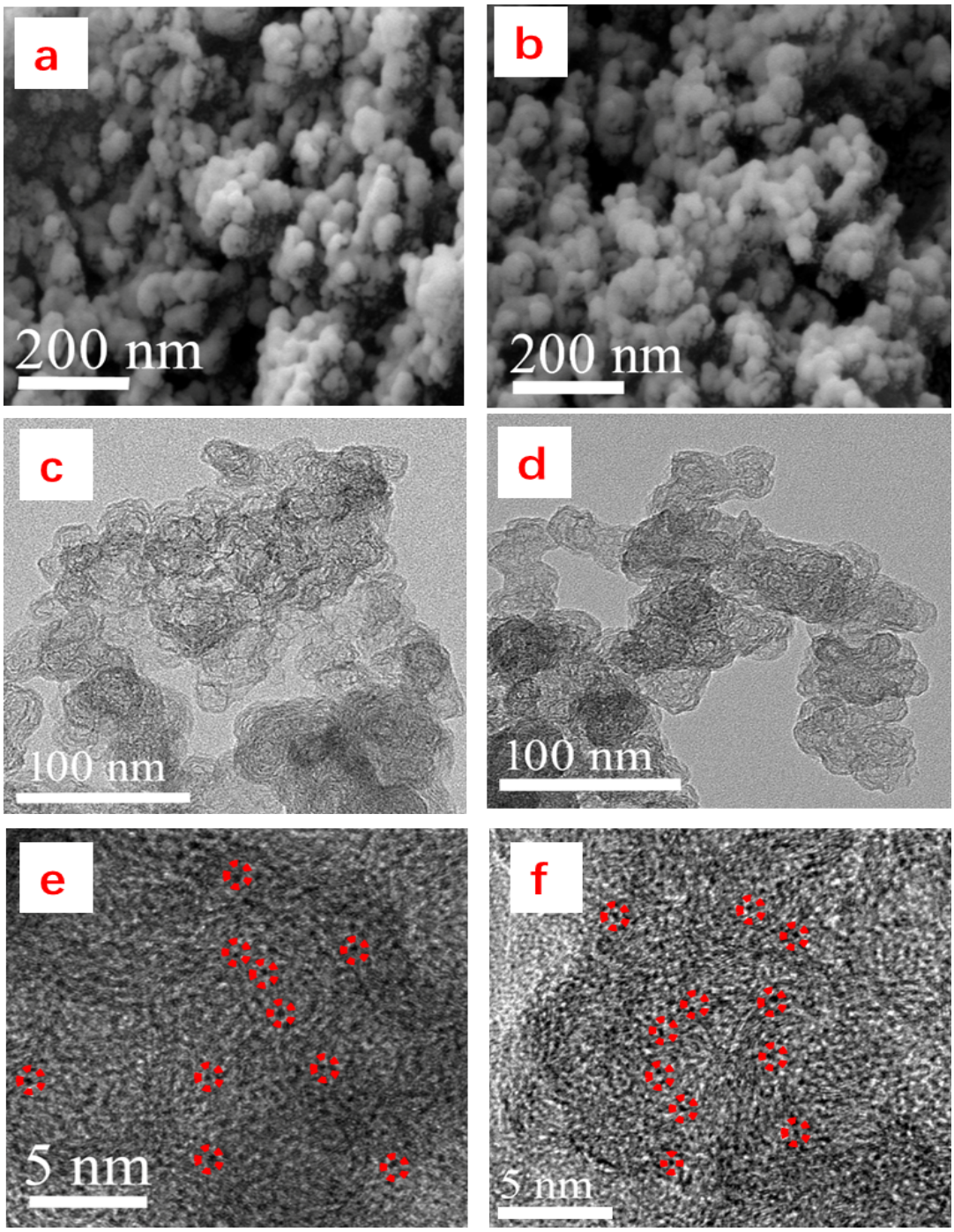

Figure S2. (a, b) SEM images of Cu-C-N and Fe-C-N catalyst samples, respectively (c, d) TEM images of Cu-C-N and Fe-C-N catalyst samples, respectively (c) HR-TEM images of Cu-C-N and Fe-C-N catalyst samples, respectively

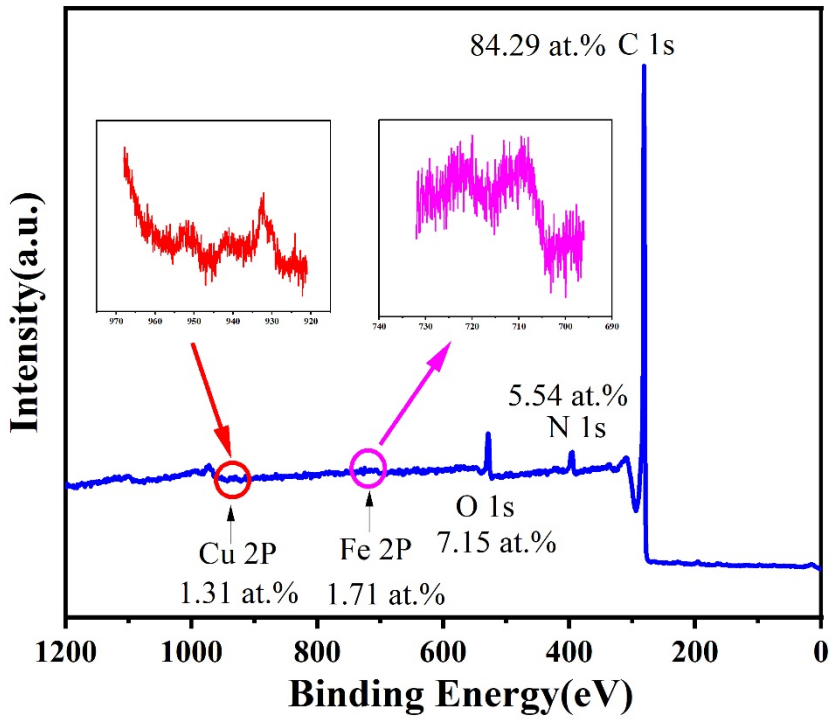

Figure S3. XPS spectra of survey spectrum for Cu-Fe-CN-3.

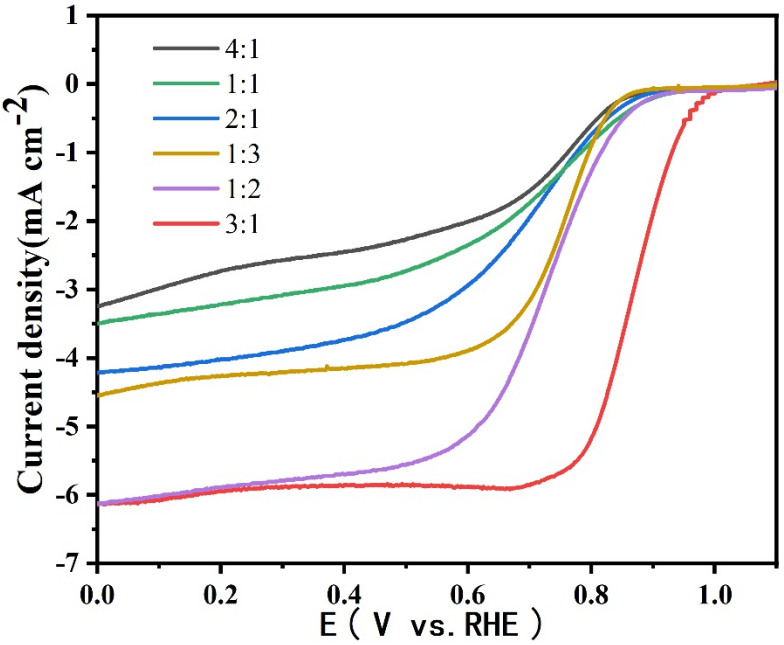

Figure S4. The linear polarization curves of air electrodes with various molar ratio of copper to iron for Cu-Fe-CN series catalysts.

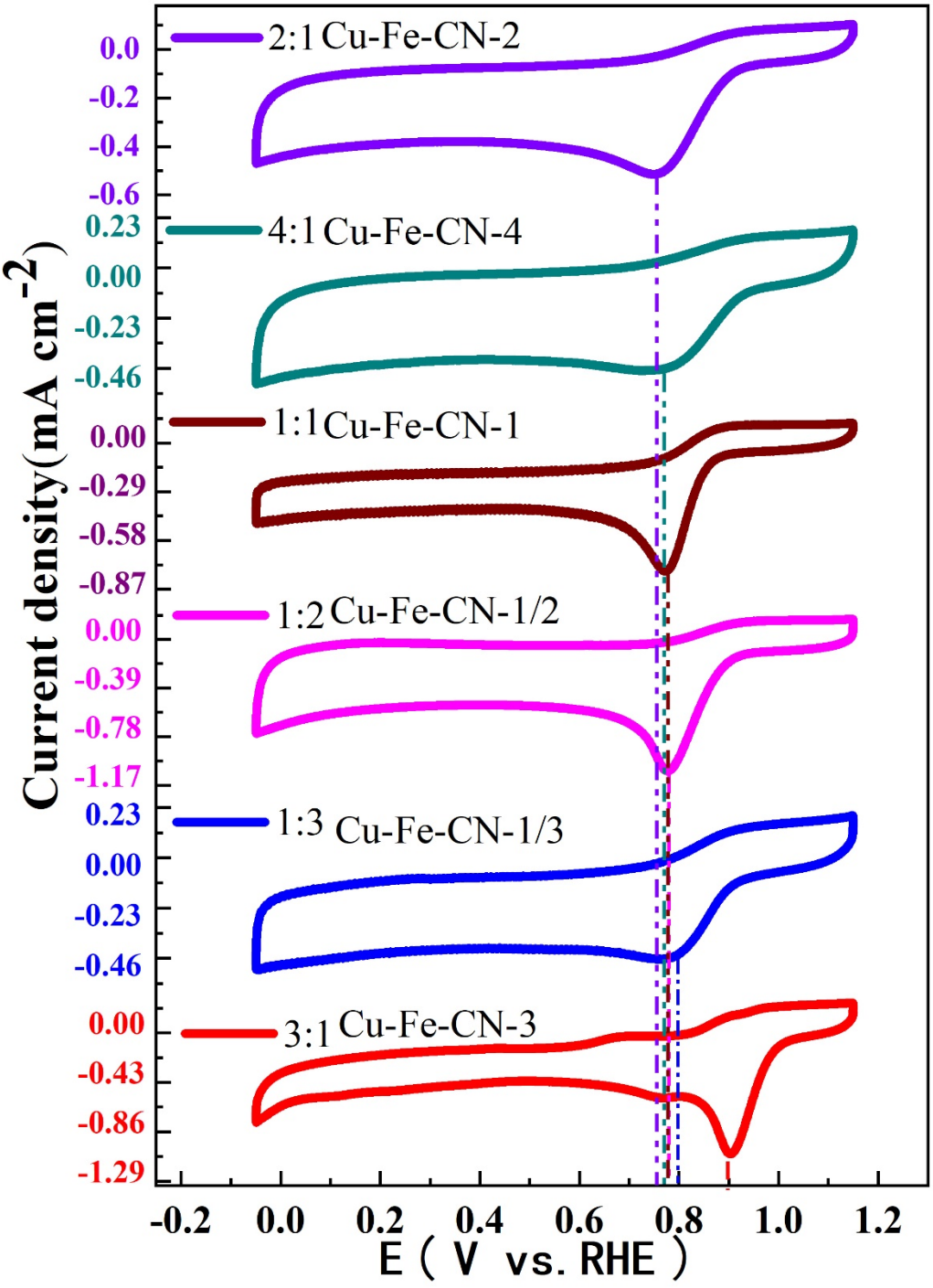

Figure S5. CV curves of samples with various molar ratio of copper to iron for Cu-Fe-CN series catalysts.

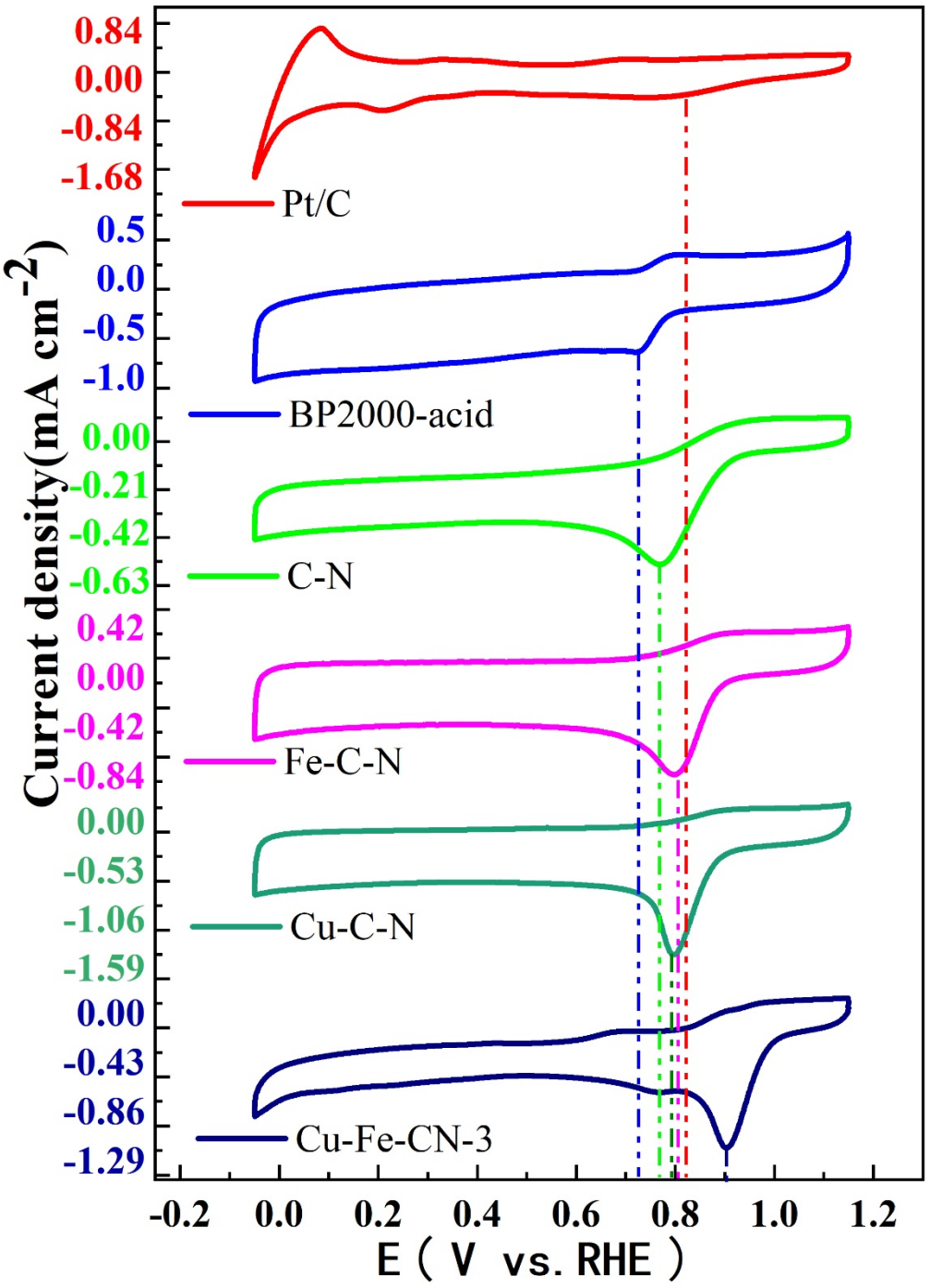

Figure S6. CV curves for different catalysts in O_2 saturated 0.1M KOH solution.

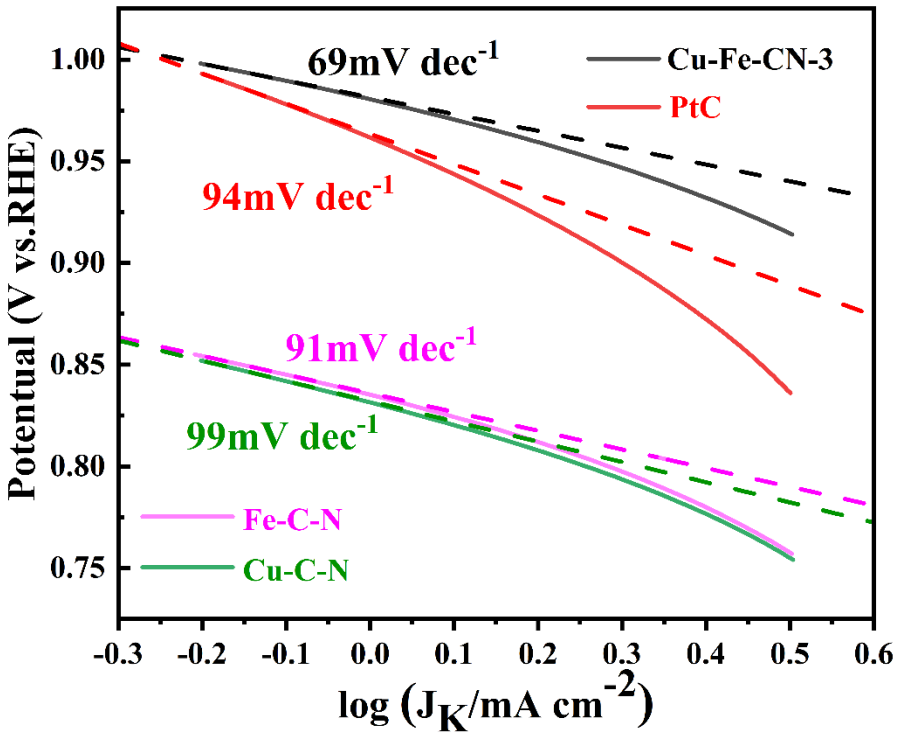

Figure S7. Tafel plots of kinetic current for Cu-C-N, Fe-C-N, Cu-Fe-CN-3 and Pt/C.

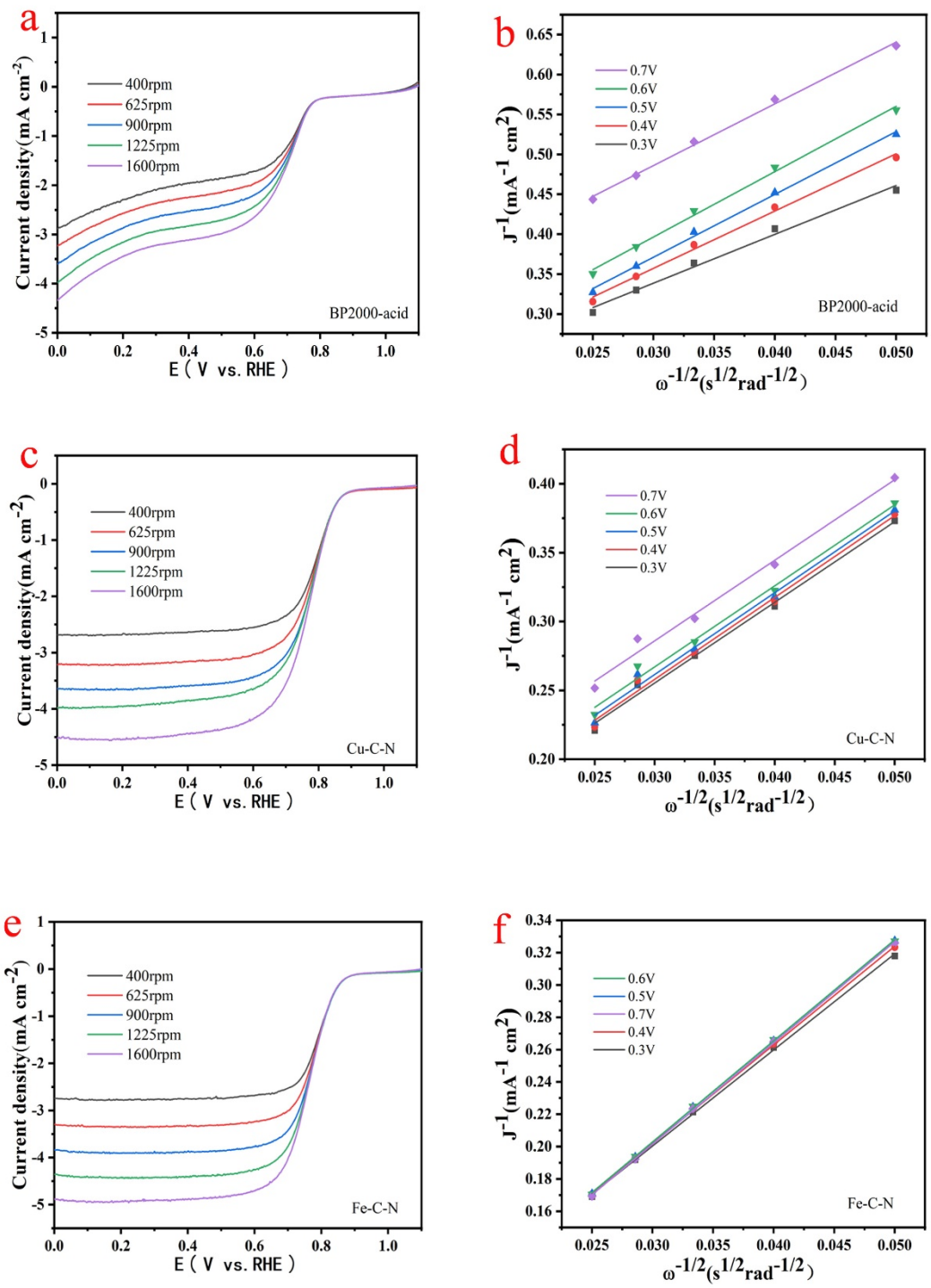

Figure S8. The RDE in O_2-saturated 0.1 M KOH solution at different rotation rates, and the corresponding Koutecky-Levich plots at different potentials of (a) and (b) BP2000-acid, (c) and (d) Cu-C-N, (e) and (f) Fe-C-N.

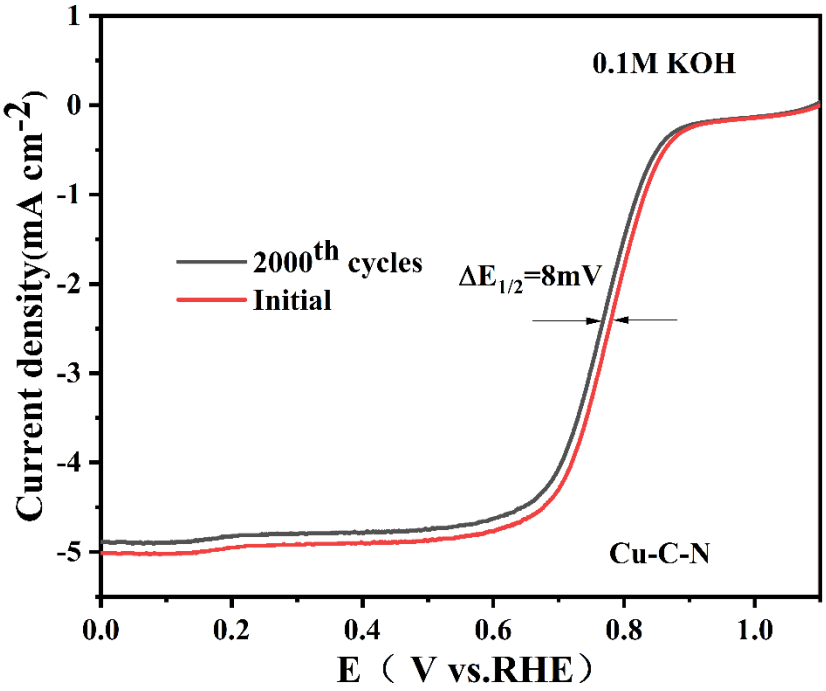

Figure S9. The ORR LSV curves of Cu-C-N before and after 2,000 cycles.

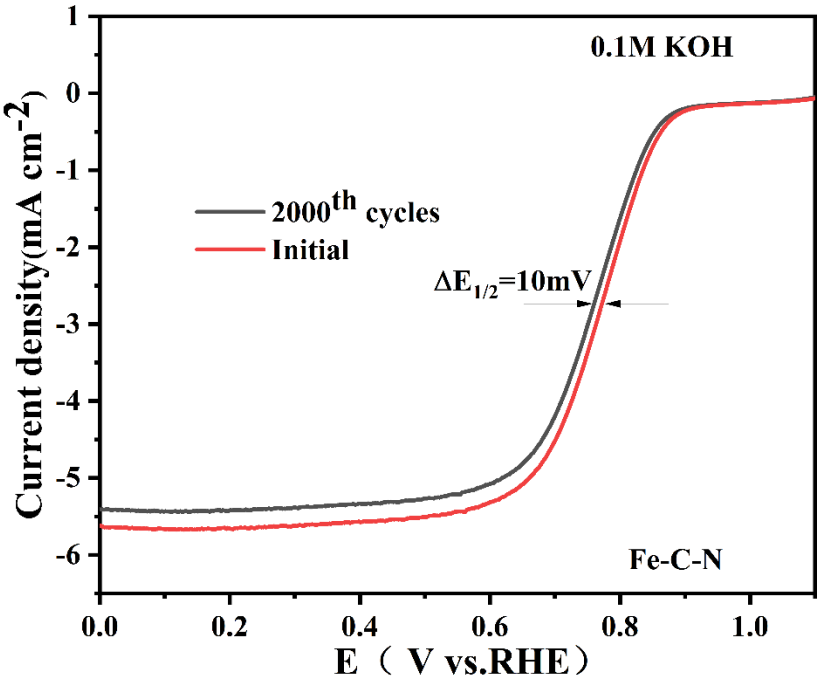

Figure S10. The ORR LSV curves of Fe-C-N before and after 2,000 cycles.

References

1 J. Li, J. Chen, H. Wan, J. Xiao, Y. Tang, M. Liu and H. Wang, *Applied Catalysis B: Environmental*, 2019, **242**, 209-217.

2. S. Zhang, Y. Wang, Y. Li, M. Wei and K. Wang, *ACS Applied Energy Materials*, 2022, **5**, 15909-15917.